THE JOURNAL OF PHYSICAL CHEMISTRY Letters

Letter

pubs.acs.org/JPCL

Methane Activation by Tantalum Carbide Cluster Anions $Ta_2C_4^-$

Hai-Fang Li,[†,‡] Yan-Xia Zhao,*[,†] Zhen Yuan,[†] Qing-Yu Liu,[†,‡] Zi-Yu Li,[†] Xiao-Na Li,[†] Chuan-Gang Ning,[§] and Sheng-Gui He*[,†]

[†]Beijing National Laboratory for Molecular Sciences, State Key Laboratory for Structural Chemistry of Unstable and Stable Species, Institute of Chemistry, Chinese Academy of Sciences, Beijing 100190, P. R. China

[‡]University of Chinese Academy of Sciences, Beijing 100049, P. R. China

[§]Department of Physics, State Key Laboratory of Low-Dimensional Quantum Physics, Tsinghua University, Beijing 100084, P. R. China

Supporting Information

ABSTRACT: Methane activation by transition metals is of fundamental interest and practical importance, as this process is extensively involved in the natural gas conversion to fuels and value-added chemicals. While single-metal centers have been well recognized as active sites for methane activation, the active center composed of two or more metal atoms is rarely addressed and the detailed reaction mechanism remains unclear. Here, by using state-of-the-art time-of-flight mass spectrometry, cryogenic anion photoelectron imaging spectroscopy, and quantum-chemical calculations, the cooperation of the two Ta atoms in a dinuclear carbide cluster $Ta_2C_4^-$ for methane activation has been identified. The C−H bond activation takes place predominantly around one Ta atom in the initial stage of the reaction and the second Ta atom accepts the delivered H atom from the C−H bond cleavage. The well-resolved vibrational spectra of the cryogenically cooled anions agree well with theoretical simulations, allowing the clear characterization of the structure of $Ta_2C_4^-$ cluster. The reactivity comparison between $Ta_2C_4^-$ cluster and the carbon-less analogues ($Ta_2C_3^-$ and $Ta_2C_2^-$) demonstrated that the cooperative effect of the two metal atoms can be well tuned by the carbon ligands in terms of methane activation and transformation.

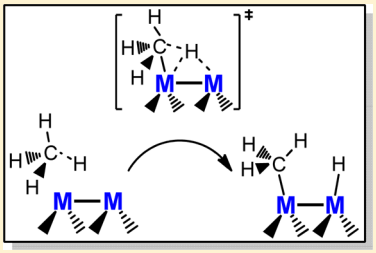

Methane, the major component of natural gas, constitutes an appealing feedstock for the synthesis of value-added chemicals and fuels.[1−3] The development of a process that would enable the efficient activation and direct conversion of methane has been a long-standing challenge because methane has strong sp^3 C−H bonds, negligible electron affinity, large ionization energy and low polarizability. Transition-metal-mediated C−H bond activation is a promising approach by which to achieve functionalization of methane.[4,5] In the reaction scenarios, it has been identified that one metal atom is generally involved in the C−H bond activation of methane.[6,7] Oxidative addition with electron-rich transition metals in low oxidation states,[8−10] electrophilic activation with electron-deficient and coordinately unsaturated transition metals in high oxidation states,[11] σ-bond metathesis with polarized metal−carbon bonds,[12] and 1,2-CH addition across a polarized metal−ligand multiple bond[13,14] have been proposed to perform the C−H bond activation in methane conversion. However, the critical role of double and multiple metal atoms, which are ubiquitous on catalytic metal surfaces as well as in transition-metal complexes, is still ambiguous for methane activation and conversion.

Recently, researchers have recognized that the cooperation of two metal atoms (e.g., Cr−Cr, Mo−Mo, Re−Re, and Sc−Sc) coordinated with supporting ligands can induce the cleavage of C−H bonds of alkenes, alkynes, and aromatics.[15−18] Hence, it is quite interesting to investigate whether the cooperative effect of two metal atoms facilitates the C−H bond activation of methane, the "Holy Grail" in chemistry. However, the complexity of condensed-phase systems[19,20] involving support, additive, and solvent effects limits the characterization of the related cooperative effect of metal atoms.

Gas-phase studies of well-defined atomic clusters under isolated, controlled, and reproducible conditions provide an important way to investigate the individual active species at the strictly molecular level.[21−25] The cooperation of a metal site and its adjacent nonmetal element, oxygen, (e.g., $Al^{\delta+}-O^{\delta-}$ and $Au^{\delta+}-O^{\delta-}$) on atomic clusters has been identified to induce the heterolytic cleavage of C−H bond of methane,[26−28] which provides the molecular-level evidence of the proposed mechanisms in many condensed-phase systems including $Mg^{2+}-O^{2-}$, $Pt^{2+}-O^{2-}$, $Pd^{2+}-O^{2-}$, $Sc^{3+}-O^{2-}$, $Al^{3+}-O^{2-}$, $Y^{3+}-O^{2-}$, and $Ln^{3+}-O^{2-}$.[29−32] The reactions of methane with bare metal clusters such as Au_2^+, $Pt_n^{\pm}$, Fe_n^+, Co_n^+, Ni_n^+, Rh_n^+, and Pd_n^+ have been frequently studied,[33−39] and the indication for methane activation by dinuclear metal centers has been provided based on the experimental observation of $M-H^+$ and $M-CH_3^+$. In this work, combined experimental and computational studies revealed that the cooperation of the two Ta atoms in a dinuclear carbide cluster $Ta_2C_4^-$ can bring about

Received: November 3, 2016
Accepted: January 15, 2017
Published: January 16, 2017

DOI: 10.1021/acs.jpclett.6b02568
J. Phys. Chem. Lett. 2017, 8, 605−610

methane activation, which further suggests that the cooperative effect of two or more metal atoms may play an important role in the activation and conversion of methane on metal-based catalysts like metal carbides and metal nanoparticles.

The time-of-flight (TOF) mass spectra for the interactions of laser ablation generated, mass-selected, and thermalized $Ta_2C_4^-$ cluster anions with CH_4, CD_4, CH_2D_2, or $^{13}CH_4$ are shown in Figure 1. As shown in Figure 1a, $Ta_2C_4^-$ can react with a trace

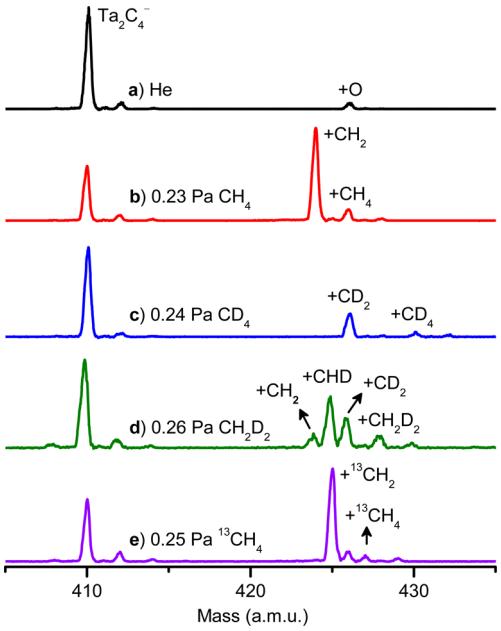

Figure 1. TOF mass spectra for the reactions of mass-selected $Ta_2C_4^-$ (a) with CH_4 (b), CD_4 (c), CH_2D_2 (d), and $^{13}CH_4$ (e) for 2.0 ms. The reactant gas pressures are shown. The label + X denotes $Ta_2C_4X^-$ (X = CH_2, CH_4, etc.).

amount of water impurity in the gas-handling system to generate $Ta_2C_4O^-$ ($Ta_2C_4^- + H_2O \rightarrow Ta_2C_4O^- + H_2$), which indicates that $Ta_2C_4^-$ is very reductive. Upon the interaction of $Ta_2C_4^-$ with 0.23 Pa CH_4 in a linear ion trap (LIT) reactor for ~2.0 ms (Figure 1b), a strong product peak assigned as $Ta_2C_5H_2^-$ was observed, suggesting the following dehydrogenation channel

$$Ta_2C_4^- + CH_4 \rightarrow Ta_2C_5H_2^- + H_2 \quad (1)$$

The isotopic labeling experiments with CD_4 (Figure 1c), CH_2D_2 (Figure 1d), and $^{13}CH_4$ (Figure 1e) confirmed the above reaction. In addition to reaction 1, minor molecular association channels generating $Ta_2C_5H_4^-$ (8%), $Ta_2C_5D_4^-$ (16%), $Ta_2C_5H_2D_2^-$ (13%), and $Ta_2C_4{}^{13}CH_4^-$ (4%) were also observed.

The experimentally generated atomic clusters can have different structural isomers with very different reactivity,[27] which can be characterized with the reactant-gas-pressure-dependent experiments (Figure S1). It turns out that (83 ± 1)% of the experimentally generated $Ta_2C_4^-$ ions were reactive toward CH_4, while the remaining component (17 ± 1)% was inert. The pseudo-first-order rate coefficient k_1 of the reactive component of $Ta_2C_4^-$ was determined to be (1.5 ± 0.5) × 10^{-11} cm^3 $molecule^{-1}$ s^{-1}. The theoretical collision rate[40,41] (k_{coll}) between $Ta_2C_4^-$ and CH_4 is calculated to be 9.3 × 10^{-10} cm^3 $molecule^{-1}$ s^{-1}, so the reaction efficiency ($\Phi = k_1/k_{coll}$) is ~1.6%. The kinetic isotopic effect (KIE)[42] defined as k_1 ($Ta_2C_4^-$ + CH_4)/k_1 ($Ta_2C_4^-$ + CD_4) amounts to 5.8 ± 1.7.

Density functional theory (DFT) calculations were carried out to investigate the structures of $Ta_2C_4^-$ cluster and the reaction mechanism with methane. With the 6-311+G (d) basis set[43] for C as well as H atoms and the effective core potential (ECP)[44] combined with the polarized triple-ζ valence (Def2-TZVP) basis set[45] for Ta atom, the bond dissociation energies (D_0) of Ta^+–CH_3, Ta^+–H, C–C, C–H, CH_3–H, H–H, Ta–Ta, and Ta^+–C were computed by various functionals and compared with available experimental data (Table S1). The TPSS functional[46] is found to be the overall best, and the computed D_0 values agree with the experimental results with an average deviation of ± 0.32 eV, and anything containing Ta has an average deviation of ± 0.21 eV. The assessment of the performance of DFT against the thermochemistry on 135 data and barrier of 38 chemical reactions[47] demonstrated that the uncertainties of TPSS predicted thermochemistry and kinetics (barriers) are 0.06 and 0.22 eV, respectively. To determine reliable relative energies of low-lying isomeric structures of $Ta_2C_4^-$ cluster, the single-point energy calculations at the high-level quantum chemistry method of coupled-cluster method with single, double, and perturbative triple excitations[48] [CCSD(T)] were performed at the TPSS-optimized geometries. Two low-lying isomers (within 0.1 eV) with doublet electronic states were determined (Figure 2 and Figure S2). An open-book structure with a Ta–Ta distance of 246 pm and two C_2 ligands symmetrically bound to their respective Ta atoms

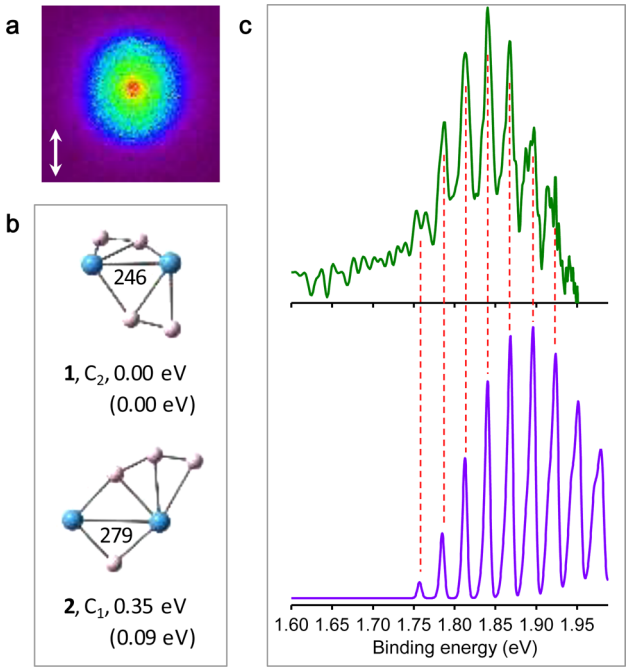

Figure 2. (a) Raw photoelectron image performed at 11 K and 636 nm. The double-headed arrow indicates the laser polarization. (b) DFT calculated structures of isomers **1** and **2** with doublet electronic states. The dihedral (open-book) angle in isomer **1** is 119.6°. The bond lengths are in pm and the relative energies at the TPSS [CCSD(T)] levels are in eV. (c) The photoelectron spectrum transformed from (a) and Franck–Condon simulated spectrum of the electronic transition $^1A \leftarrow {}^2A$ for isomer **1** shown as green and purple traces, respectively. The simulated spectrum is blue-shifted by 0.175 eV to align with the experimental vibrational origin (see details in Figure S4).

DOI: 10.1021/acs.jpclett.6b02568
J. Phys. Chem. Lett. 2017, 8, 605–610

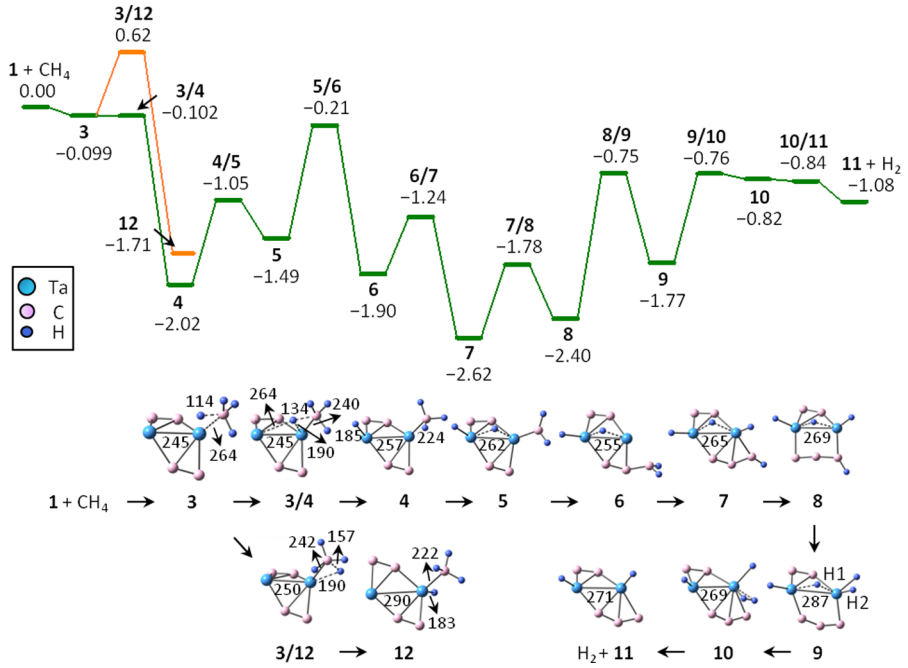

Figure 3. DFT-calculated potential-energy profile for reaction of $Ta_2C_4^-$ (isomer **1**) with CH_4 in doublet spin state. The relative energies (ΔH_0 in eV) of the reaction intermediates, transition states, and products with respect to the separated reactants are given. Bond lengths are given in pm. The structures of the transition states **4/5**−**10/11** are shown in Figure S5.

(**1**, Figure 2b) is slightly more stable than the asymmetric quasi-planar isomer (**2**, Figure 2b). This result well supports the experimental suggestion that the generated $Ta_2C_4^-$ clusters do not have a uniform structure populated in the LIT reactor.

Cryogenic anion photoelectron imaging spectroscopy[49,50] was employed to study the vibrational and geometric structures specific to the $Ta_2C_4^-$ cluster at 11 K (Figure 2c). A well-resolved vibrational progression with a peak spacing of 222 ± 4 cm^{-1} has been observed (green spectrum). This spectrum is in agreement with the Franck−Condon simulated profile of the $^1A \leftarrow {}^2A$ transition for isomer **1** (a peak spacing of 224 ± 1 cm^{-1}, purple spectrum). When the typical peak spacing is compared with the calculated frequencies of the neutral Ta_2C_4 (Table S2), the best agreement comes with ∼225 cm^{-1} for an in-plane vibration of the two C_2 ligands (Figure S3). The resolved vibrational transitions are then assigned to the 11_0^n progression. The adiabatic detachment energy (ADE) of isomer **1** is experimentally given to be 1.76 ± 0.01 eV, which is the onset of the one-photon detachment from $Ta_2C_4^-$.

Isomer **2** is calculated to have a congested spectrum with ADE of 2.02 eV. In the photoelectron spectrum recorded at a wavelength of 420 nm, due to the weak transition of $^1A \leftarrow {}^2A$ for isomer **2** and low abundance of this species, there is no discernible vibrational band to feature this structure at the high electron binding energy region (see more details in Figure S4). Considering the high abundance (83%) of the active $Ta_2C_4^-$ in the reactivity experiments, it is concluded that the lowest-lying structure of $Ta_2C_4^-$ cluster corresponds to isomer **1**.

The DFT-calculated reaction mechanism for the reaction of $Ta_2C_4^-$ (isomer **1**) with methane is shown in Figure 3 along the doublet potential energy surface. Either of the equivalent Ta atoms (0.36 e, natural charge) in $Ta_2C_4^-$ can trap methane to form the encounter complex **3**. In this process, one C−H bond of methane is apparently preactivated, as can be seen from the elongation of the C−H distance from 109 pm in free CH_4 to 114 pm in intermediate **3**. Then, the preactivated C−H bond of methane is cleaved around two Ta atoms via a transition state (**3/4**), leading to barrier-free formation of **4**. The resulting intermediate **4** with a smaller Ta−Ta Wiberg bond order of 1.6 has a longer Ta−Ta bond length of 257 pm when compared with the values for the methane adduct **3** (2.1 and 245 pm of Ta−Ta bond order and bond length, respectively).

The subsequent step requires activation of a second C−H bond of CH_4 to generate a metal carbene complex **5** (**4** → **5**). After C−C bond coupling (**5** → **6**), the consecutive cleavages of two other C−H bonds (**6** → **7** and **8** → **9**) lead to the formation of intermediate **9** with four H atoms coordinated to two metal sites from which a H_2 unit can be formed by combining two H atoms (H1 and H2, **9** → **10**). The resulting intermediate **10** can easily evaporate the formed H_2 moiety to produce the experimentally observed $Ta_2C_5H_2^-$ product (Figure 1, see the detailed discussion about the relative energies of **10**, **10/11**, and **11**+H_2 in Figure S5). All of the reaction intermediates and transition states shown in Figure 3 are lower in energy than the separated reactants, indicating that methane dehydrogenation by isomer **1** is thermodynamically and kinetically favorable if the first C−H bond is cleaved around two metal atoms.

Molecular orbital (MO) analysis for the interaction between $Ta_2C_4^-$ (isomer **1**) and CH_4 has been performed (Figure S6) to obtain further insight into the detailed reaction mechanism of methane activation. The symmetry matching between MOs of CH_4 and a single-Ta atom in $Ta_2C_4^-$ demonstrates that the C−H bond activation of methane primarily occurs at a single-metal center in the initial stage of the reaction, which is supported by the geometrical characteristics of transition state **3/4** that the C−H bond being broken is not located over the Ta−Ta bond, rather it is centered over a single Ta atom (Figure 3). Despite the fact that the single-Ta atom plays a crucial role in the initial stage of methane activation, the importance of the second Ta atom in cleavage of the C−H bond should also attract attention because the second Ta atom allows the H atom formed to

DOI: 10.1021/acs.jpclett.6b02568
J. Phys. Chem. Lett. 2017, 8, 605−610

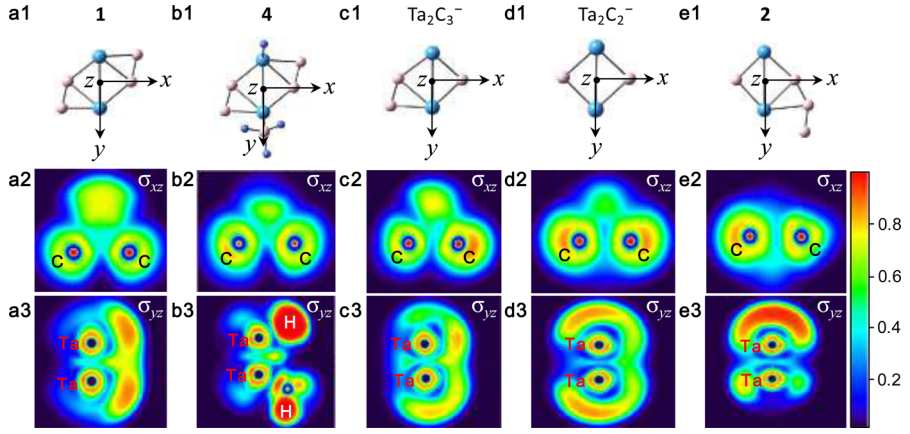

Figure 4. Two-dimensional ELFs of the reactive $Ta_2C_4^-$ and reaction intermediate **4** are shown in (a) and (b), respectively. The unreactive $Ta_2C_3^-$, $Ta_2C_2^-$ and isomer **2** are also presented for comparison (c−e). The ELF distributions are shown on two planes of σ_{xz} and σ_{yz} (σ_{xz} intersects two C atoms and σ_{yz} intersects two Ta atoms) and are described chromatically. A large ELF value means that electrons are greatly localized.

migrate away from the single-Ta center driven by the thermodynamics. The important role of the second Ta atom can be further confirmed by the reaction kinetics for C−H bond cleavage occurring at a single-metal center. On the basis of orbital analysis, all valence electrons of the Ta atom have been used to bond with C atoms and the other Ta atom. As a result, no lone electron pair locates at any of the Ta atoms, and the oxidative addition[51,52] of one C−H bond to a single-Ta center is subject to a positive barrier of 0.62 eV (**3**/**12**, Figure 3), indicating that this pathway can be excluded under thermal collision conditions.[53] It is noteworthy that thermal C−H activation by the Ta−C centers is also kinetically unfavorable (Figure S7). Thus methane activation facilitated by the cooperation of the two Ta atoms is identified for the reaction with $Ta_2C_4^-$ cluster (isomer **1**). The reaction of isomer **2** with methane is subject to positive barriers for C−H bond cleavage around either one or two Ta atoms (≥0.21 eV, Figure S8), implying that isomer **2** could be the unreactive component of $Ta_2C_4^-$ in the experiments.

To explore the excellent ability of the cooperative two metal atoms in the reactive $Ta_2C_4^-$ isomer to promote methane activation, the reactions of one- and two-carbon-less clusters, $Ta_2C_3^-$ and $Ta_2C_2^-$, with methane have also been studied. No reactivity ($k_1 < 10^{-14}$ cm^3 molecule^{-1} s^{-1}, the detection limit) was observed in the experiments, and the DFT calculations also predicted overall positive barriers for C−H bond activation by the cooperation of the two Ta atoms in the two clusters (≥0.27 eV, Figures S9 and S10). The electronic nature of the two metal atoms has been analyzed at DFT level by means of topological analysis of the electron localization functions (ELFs).[54] ELF shows a significant decrease in electron density among the two Ta atoms in $Ta_2C_4^-$ after C−H bond cleavage (Figures 4a, b), implying that both of the two Ta atoms participate in the overall C−H bond cleavage of methane (**3** → **3**/**4** → **4**, Figure 3). The donation of two electrons from the metal d orbitals to the C−H antibonding orbital is the driving force for the C−H bond cleavage of methane.[55,56] As a result, the two electrons in the reactive $Ta_2C_4^-$ are stored in the two metal atoms, and the process of C−H bond cleavage is accompanied by a formal one-electron oxidation[20,57] of each Ta atom with a corresponding reduction in the Ta−Ta bond order from 2.1 to 1.6. The comparison of the ELF distributions in Figure 4a,c−e shows that the electron density stored in the two Ta atoms of the reactive $Ta_2C_4^-$ isomer is significantly greater than that in both the unreactive $Ta_2C_4^-$ isomer and carbon-less analogues. The trend of the decrease in the electron density stored in the two Ta atoms in $Ta_2C_4^-$, $Ta_2C_3^-$, and $Ta_2C_2^-$ clusters correlates well with an increase in activation barriers when the clusters are reacted with methane (−0.10, 0.27, and 0.65 eV for $Ta_2C_4^-$, $Ta_2C_3^-$, and $Ta_2C_2^-$, respectively). These results clearly indicate the reactivity difference of the cooperative two metal atoms surrounded by different ligands.[58]

The symmetrical C_2 ligands in $Ta_2C_4^-$ cluster afford an electron-rich dinuclear metal center over which the C−H bond of methane is cleaved in a homolytic manner. However, when one or both of the two C_2 ligands is replaced with the C_1 ligands to form $Ta_2C_3^-$ or $Ta_2C_2^-$, the cooperative effect of the two Ta atoms decreases quickly toward methane. Similarly, the two Ta centers coordinated with one C_1 and one C_3 ligand in the unreactive $Ta_2C_4^-$ (isomer **2**) are also identified to be inert. These results suggest that the presence of symmetrical C_2 ligands (bond order of ∼2) with π-donating ability[59] can facilitate the cooperative effect of the two Ta atoms mediated in C−H bond activation.

In conclusion, complementary mass spectrometry, photoelectron imaging spectroscopy, and first-principles calculations allowed us to identify the mechanism of methane activation by the cooperation of the two Ta atoms in a tantalum carbide cluster $Ta_2C_4^-$. Symmetrical C_2 ligands play an important role in enhancing the reactivity of the dinuclear metal species. This study has provided important insight regarding the activation and conversion of methane on metal carbides and metal nanoparticles.

■ ASSOCIATED CONTENT

Ⓢ Supporting Information

The Supporting Information is available free of charge on the ACS Publications website at DOI: 10.1021/acs.jpclett.6b02568.

Details regarding experimental and theoretical methods, TOF mass spectra, experimental reaction kinetics, photoelectron spectroscopy, computational results, and data analysis. (PDF)

■ AUTHOR INFORMATION

Corresponding Authors

*Y.-X.Z.: E-mail: chemzyx@iccas.ac.cn.

DOI: 10.1021/acs.jpclett.6b02568
J. Phys. Chem. Lett. 2017, 8, 605−610

*S.-G.H.: E-mail: shengguihe@iccas.ac.cn. Phone: +86-10-62568330. Fax: +86-10-62559373.

ORCID

Sheng-Gui He: 0000-0002-9919-6909

Notes

The authors declare no competing financial interest.

■ ACKNOWLEDGMENTS

This work was financially supported by the Chinese Academy of Sciences (No. XDA09030101), the National Natural Science Foundation of China (Nos. 21273247, 21325314, and 91645203), and the Major Research Plan of China (No. 2013CB834603). The support from the referees pointing out relevant literature references and making very helpful comments is acknowledged.

■ REFERENCES

(1) Guo, X.; Fang, G.; Li, G.; Ma, H.; Fan, H.; Yu, L.; Ma, C.; Wu, X.; Deng, D.; Wei, M.; et al. Direct, Nonoxidative Conversion of Methane to Ethylene, Aromatics, and Hydrogen. *Science* **2014**, *344*, 616−619.

(2) Peter, M.; Marks, T. J. Platinum Metal-Free Catalysts for Selective Soft Oxidative Methane → Ethylene Coupling. Scope and Mechanistic Observations. *J. Am. Chem. Soc.* **2015**, *137*, 15234−15240.

(3) Crabtree, R. H. Aspects of Methane Chemistry. *Chem. Rev.* **1995**, *95*, 987−1007.

(4) Horn, R.; Schlögl, R. Methane Activation by Heterogeneous Catalysis. *Catal. Lett.* **2015**, *145*, 23−39.

(5) Alvarez-Galvan, M. C.; Mota, N.; Ojeda, M.; Rojas, S.; Navarro, R. M.; Fierro, J. L. G. Direct Methane Conversion Routes to Chemicals and Fuels. *Catal. Today* **2011**, *171*, 15−23.

(6) Caballero, A.; Perez, P. J. Methane as Raw Material in Synthetic Chemistry: The Final Frontier. *Chem. Soc. Rev.* **2013**, *42*, 8809−8820.

(7) Cavaliere, V. N.; Mindiola, D. J. Methane: A New Frontier in Organometallic Chemistry. *Chem. Sci.* **2012**, *3*, 3356−3365.

(8) Bergman, R. G. Activation of Alkanes with Organotransition Metal Complexes. *Science* **1984**, *223*, 902−908.

(9) Hoyano, J. K.; McMaster, A. D.; Graham, W. A. G. Activation of Methane by Iridium Complexes. *J. Am. Chem. Soc.* **1983**, *105*, 7190−7191.

(10) Luecke, H. F.; Bergman, R. G. Synthesis and C−H Activation Reactions of Cyclometalated Complexes of Ir(III): $Cp^*(PMe_3)Ir(CH_3)^+$ Does Not Undergo Intermolecular C−H Activation in Solution via a Cyclometalated Intermediate. *J. Am. Chem. Soc.* **1997**, *119*, 11538−11539.

(11) Periana, R. A.; Mironov, O.; Taube, D.; Bhalla, G.; Jones, C. Catalytic, Oxidative Condensation of CH_4 to CH_3COOH in One Step via CH Activation. *Science* **2003**, *301*, 814−818.

(12) Fendrick, C. M.; Marks, T. J. Thermochemically Based Strategies for Carbon-Hydrogen Activation on Saturated Hydrocarbon Molecules. Ring-Opening Reactions of a Thoracyclobutane with Tetramethylsilane and Methane. *J. Am. Chem. Soc.* **1984**, *106*, 2214−2216.

(13) Cummins, C. C.; Baxter, S. M.; Wolczanski, P. T. Methane and Benzene Activation via Transient $(tert\text{-}Bu_3SiNH)_2Zr{:}NSi\text{-}tert\text{-}Bu_3$. *J. Am. Chem. Soc.* **1988**, *110*, 8731−8733.

(14) Gao, J.; Zheng, Y.; Jehng, J.-M.; Tang, Y.; Wachs, I. E.; Podkolzin, S. G. Identification of Molybdenum Oxide Nanostructures on Zeolites for Natural Gas Conversion. *Science* **2015**, *348*, 686−690.

(15) Noor, A.; Sobgwi Tamne, E.; Qayyum, S.; Bauer, T.; Kempe, R. Cycloaddition Reactions of a Chromium−Chromium Quintuple Bond. *Chem. - Eur. J.* **2011**, *17*, 6900−6903.

(16) Chen, H.-Z.; Liu, S.-C.; Yen, C.-H.; Yu, J.-S. K.; Shieh, Y.-J.; Kuo, T.-S.; Tsai, Y.-C. Reactions of Metal−Metal Quintuple Bonds with Alkynes: [2 + 2+2] and [2 + 2] Cycloadditions. *Angew. Chem., Int. Ed.* **2012**, *51*, 10342−10346.

(17) Adams, R. D.; Rassolov, V.; Wong, Y. O. Binuclear Aromatic C−H Bond Activation at a Dirhenium Site. *Angew. Chem., Int. Ed.* **2016**, *55*, 1324−1327.

(18) Huang, W.; Dulong, F.; Khan, S. I.; Cantat, T.; Diaconescu, P. L. Bimetallic Cleavage of Aromatic C−H Bonds by Rare-Earth-Metal Complexes. *J. Am. Chem. Soc.* **2014**, *136*, 17410−17413.

(19) Karakaya, C.; Kee, R. J. Progress in the Direct Catalytic Conversion of Methane to Fuels and Chemicals. *Prog. Energy Combust. Sci.* **2016**, *55*, 60−97.

(20) Olivos-Suarez, A. I.; Szécsényi, À.; Hensen, E. J. M.; Ruiz-Martinez, J.; Pidko, E. A.; Gascon, J. Strategies for the Direct Catalytic Valorization of Methane Using Heterogeneous Catalysis: Challenges and Opportunities. *ACS Catal.* **2016**, *6*, 2965−2981.

(21) Johnson, G. E.; Tyo, E. C.; Castleman, A. W. Cluster Reactivity Experiments: Employing Mass Spectrometry to Investigate the Molecular Level Details of Catalytic Oxidation Reactions. *Proc. Natl. Acad. Sci. U. S. A.* **2008**, *105*, 18108−18113.

(22) Böhme, D. K.; Schwarz, H. Gas-Phase Catalysis by Atomic and Cluster Metal Ions: The Ultimate Single-Site Catalysts. *Angew. Chem., Int. Ed.* **2005**, *44*, 2336−2354.

(23) O'Hair, R. J.; Khairallah, G. Gas Phase Ion Chemistry of Transition Metal Clusters: Production, Reactivity, and Catalysis. *J. Cluster Sci.* **2004**, *15*, 331−363.

(24) Gong, Y.; Zhou, M.; Andrews, L. Spectroscopic and Theoretical Studies of Transition Metal Oxides and Dioxygen Complexes. *Chem. Rev.* **2009**, *109*, 6765−6808.

(25) Ding, X.-L.; Wu, X.-N.; Zhao, Y.-X.; He, S.-G. C−H Bond Activation by Oxygen-Centered Radicals over Atomic Clusters. *Acc. Chem. Res.* **2012**, *45*, 382−390.

(26) Li, J.; Zhou, S.; Zhang, J.; Schlangen, M.; Usharani, D.; Shaik, S.; Schwarz, H. Mechanistic Variants in Gas-Phase Metal-Oxide Mediated Activation of Methane at Ambient Conditions. *J. Am. Chem. Soc.* **2016**, *138*, 11368−11377.

(27) Li, Z.-Y.; Li, H.-F.; Zhao, Y.-X.; He, S.-G. Gold(III) Mediated Activation and Transformation of Methane on Au_1-Doped Vanadium Oxide Cluster Cations $AuV_2O_6^+$. *J. Am. Chem. Soc.* **2016**, *138*, 9437−9443.

(28) Zhao, Y.-X.; Li, X.-N.; Yuan, Z.; Liu, Q.-Y.; Shi, Q.; He, S.-G. Methane Activation by Gold-Doped Titanium Oxide Cluster Anions with Closed-Shell Electronic Structures. *Chem. Sci.* **2016**, *7*, 4730−4735.

(29) Ito, T.; Tashiro, T.; Kawasaki, M.; Watanabe, T.; Toi, K.; Kobayashi, H. Adsorption of Methane on Magnesium Oxide Studied by Temperature-Programmed Desorption and Ab Initio Molecular Orbital Methods. *J. Phys. Chem.* **1991**, *95*, 4476−4483.

(30) Vedernikov, A. N. Direct Functionalization of M−C (M = Pt^{II}, Pd^{II}) Bonds Using Environmentally Benign Oxidants, O_2 and H_2O_2. *Acc. Chem. Res.* **2012**, *45*, 803−813.

(31) Burch, R.; Hayes, M. J. C−H bond Activation in Hydrocarbon Oxidation on Solid Catalysts. *J. Mol. Catal. A: Chem.* **1995**, *100*, 13−33.

(32) Podkolzin, S. G.; Stangland, E. E.; Jones, M. E.; Peringer, E.; Lercher, J. A. Methyl Chloride Production from Methane over Lanthanum-Based Catalysts. *J. Am. Chem. Soc.* **2007**, *129*, 2569−2576.

(33) Lang, S. M.; Bernhardt, T. M.; Barnett, R. N.; Landman, U. Methane Activation and Catalytic Ethylene Formation on Free Au_2^+. *Angew. Chem., Int. Ed.* **2010**, *49*, 980−983.

(34) Kummerlöwe, G.; Balteanu, I.; Sun, Z.; Balaj, O. P.; Bondybey, V. E.; Beyer, M. K. Activation of Methane and Methane-d_4 by Ionic Platinum Clusters. *Int. J. Mass Spectrom.* **2006**, *254*, 183−188.

(35) Liyanage, R.; Zhang, X.-G.; Armentrout, P. B. Activation of Methane by Size-Selected Iron Cluster Cations, Fe_n^+ (n = 2−15): Cluster-CH_x (x = 0−3) Bond Energies and Reaction Mechanisms. *J. Chem. Phys.* **2001**, *115*, 9747−9763.

(36) Citir, M.; Liu, F.; Armentrout, P. B. Methane Activation by Cobalt Cluster Cations, Co_n^+ (n = 2−16): Reaction Mechanisms and Thermochemistry of Cluster-CH_x (x = 0−3) Complexes. *J. Chem. Phys.* **2009**, *130*, 054309.

DOI: 10.1021/acs.jpclett.6b02568
J. Phys. Chem. Lett. 2017, 8, 605−610

(37) Liu, F.; Zhang, X.-G.; Liyanage, R.; Armentrout, P. B. Methane Activation by Nickel Cluster Cations, Ni_n^+ (n = 2−16): Reaction Mechanisms and Thermochemistry of Cluster-CH_x (x = 0−3) Complexes. *J. Chem. Phys.* **2004**, *121*, 10976−10990.
(38) Albert, G.; Berg, C.; Beyer, M.; Achatz, U.; Joos, S.; Niedner-Schatteburg, G.; Bondybey, V. E. Methane Activation by Rhodium Cluster Argon Complexes. *Chem. Phys. Lett.* **1997**, *268*, 235−241.
(39) Lang, S. M.; Frank, A.; Bernhardt, T. M. Activation and Catalytic Dehydrogenation of Methane on Small Pd_x^+ and Pd_xO^+ Clusters. *J. Phys. Chem. C* **2013**, *117*, 9791−9800.
(40) Gioumousis, G.; Stevenson, D. P. Reactions of Gaseous Molecule Ions with Gaseous Molecules. V. Theory. *J. Chem. Phys.* **1958**, *29*, 294−299.
(41) Kummerlöwe, G.; Beyer, M. K. Rate Estimates for Collisions of Ionic Clusters with Neutral Reactant Molecules. *Int. J. Mass Spectrom.* **2005**, *244*, 84−90.
(42) Schröder, D.; Schwarz, H. Gas-Phase Activation of Methane by Ligated Transition-Metal Cations. *Proc. Natl. Acad. Sci. U. S. A.* **2008**, *105*, 18114−18119.
(43) Krishnan, R.; Binkley, J. S.; Seeger, R.; Pople, J. A. Self-Consistent Molecular Orbital Methods. XX. A Basis Set for Correlated Wave Functions. *J. Chem. Phys.* **1980**, *72*, 650−654.
(44) Andrae, D.; Häußermann, U.; Dolg, M.; Stoll, H.; Preuß, H. Energy-Adjustedab Initio Pseudopotentials for the Second and Third Row Transition Elements. *Theor. Chim. Acta* **1990**, *77*, 123−141.
(45) Weigend, F.; Ahlrichs, R. Balanced Basis Sets of Split Valence, Triple Zeta Valence and Quadruple Zeta Valence Quality for H to Rn: Design and Assessment of Accuracy. *Phys. Chem. Chem. Phys.* **2005**, *7*, 3297−3305.
(46) Tao, J.; Perdew, J. P.; Staroverov, V. N.; Scuseria, G. E. Climbing the Density Functional Ladder: Nonempirical Meta-Generalized Gradient Approximation Designed for Molecules and Solids. *Phys. Rev. Lett.* **2003**, *91*, 146401.
(47) Zhao, Y.; Schultz, N. E.; Truhlar, D. G. Exchange-Correlation Functional with Broad Accuracy for Metallic and Nonmetallic Compounds, Kinetics, and Noncovalent Interactions. *J. Chem. Phys.* **2005**, *123*, 161103.
(48) Watts, J. D.; Gauss, J.; Bartlett, R. J. Coupled-Cluster Methods with Noniterative Triple Excitations for Restricted Open-Shell Hartree-Fock and Other General Single Determinant Reference Functions. Energies and Analytical Gradients. *J. Chem. Phys.* **1993**, *98*, 8718−8733.
(49) Kim, J. B.; Weichman, M. L.; Neumark, D. M. Structural Isomers of Ti_2O_4 and Zr_2O_4 Anions Identified by Slow Photoelectron Velocity-Map Imaging Spectroscopy. *J. Am. Chem. Soc.* **2014**, *136*, 7159−7168.
(50) Hrovat, D. A.; Hou, G.-L.; Wang, X.-B.; Borden, W. T. Negative Ion Photoelectron Spectroscopy Confirms the Prediction that 1,2,4,5-Tetraoxatetramethylenebenzene Has a Singlet Ground State. *J. Am. Chem. Soc.* **2015**, *137*, 9094−9099.
(51) Li, H.-F.; Li, Z.-Y.; Liu, Q.-Y.; Li, X.-N.; Zhao, Y.-X.; He, S.-G. Methane Activation by Iron-Carbide Cluster Anions FeC_6^-. *J. Phys. Chem. Lett.* **2015**, *6*, 2287−2291.
(52) Ma, J.-B.; Xu, L.-L.; Liu, Q.-Y.; He, S.-G. Activation of Methane and Ethane as Mediated by the Triatomic Anion $HNbN^-$: Electronic Structure Similarity with a Pt Atom. *Angew. Chem., Int. Ed.* **2016**, *55*, 4947−4951.
(53) Yuan, Z.; Li, Z.-Y.; Zhou, Z.-X.; Liu, Q.-Y.; Zhao, Y.-X.; He, S.-G. Thermal Reactions of $(V_2O_5)_nO^-$ (n = 1−3) Cluster Anions with Ethylene and Propylene: Oxygen Atom Transfer Versus Molecular Association. *J. Phys. Chem. C* **2014**, *118*, 14967−14976.
(54) Butovskii, M. V.; Döring, C.; Bezugly, V.; Wagner, F. R.; Grin, Y.; Kempe, R. Molecules Containing Rare-Earth Atoms Solely Bonded by Transition Metals. *Nat. Chem.* **2010**, *2*, 741−744.
(55) Li, Z.-Y.; Hu, L.; Liu, Q.-Y.; Ning, C.-G.; Chen, H.; He, S.-G.; Yao, J. C−H Bond Activation by Early Transition Metal Carbide Cluster Anion MoC_3^-. *Chem. - Eur. J.* **2015**, *21*, 17748−17756.
(56) Zhou, S.; Li, J.; Schlangen, M.; Schwarz, H. Bond Activation by Metal-Carbene Complexes in the Gas Phase. *Acc. Chem. Res.* **2016**, *49*, 494−502.
(57) Powers, I. G.; Uyeda, C. Metal−Metal Bonds in Catalysis. *ACS Catal.* **2016**, *7*, 936−958.
(58) Steiman, T. J.; Uyeda, C. Reversible Substrate Activation and Catalysis at an Intact Metal−Metal Bond Using a Redox-Active Supporting Ligand. *J. Am. Chem. Soc.* **2015**, *137*, 6104−6110.
(59) Wang, D. Y.; Choliy, Y.; Haibach, M. C.; Hartwig, J. F.; Krogh-Jespersen, K.; Goldman, A. S. Assessment of the Electronic Factors Determining the Thermodynamics of ″Oxidative Addition″ of C−H and N−H Bonds to Ir(I) Complexes. *J. Am. Chem. Soc.* **2016**, *138*, 149−163.

DOI: 10.1021/acs.jpclett.6b02568
J. Phys. Chem. Lett. 2017, 8, 605−610